

Ethylene Tri- and Tetramerization: a Steric Parameter Selectivity Switch from X-ray Crystallography and Computational Analysis

Nicoline Cloete,[†] Hendrik G. Visser,^{*,‡} Ilana Engelbrecht,[‡] Matthew J. Overett,[†] William F. Gabrielli,[†] and Andreas Roodt^{*,‡}[†]R&D Division, SASOL Technology (Pty) Ltd., 1 Klasie Havenga Road, Sasolburg, South Africa[‡]Department of Chemistry, University of the Free State, Nelson Mandela Avenue, Bloemfontein, South Africa

Supporting Information

ABSTRACT: A steric parameter ($\theta_{N\text{-sub}}$) is introduced to describe the steric bulk at the nitrogen atom on a range of PNP ligands used in ethylene tri- and tetramerization. This parameter was calculated for the free ligands and different metal complexes thereof and compared to catalytic data. A specific tendency is observed for the value of $\theta_{N\text{-sub}}$ and 1-hexene selectivity, and a slight increase in 1-octene selectivity is found with increased bulkiness of the substituents on the nitrogen atom.

There is a worldwide need to develop a systematic approach toward the design of molecular systems such as catalysts and pharmaceuticals of interest to industry, as opposed to the random hit-and-run approach usually adopted because of financial constraints. Short-chain linear α -olefins (LAOs), such as 1-hexene and 1-octene, are used as comonomers in the production of linear low-density polyethylene. The selective trimerization of ethylene to 1-hexene is well-established, and several large companies, such as Phillips (pyrollide system), SASOL (mixed heteroatomic systems), and BP (diphosphine systems), developed effective catalysts for this.¹ However, until recently, the corresponding tetramerization process to yield 1-octene was unknown. The first catalyst system capable of yielding 1-octene in unexpected high selectivity (70%) was reported in 2004.² The active catalyst is produced in situ by the addition of methylaluminoxane to a mixture of a bidentate diphosphinoamine and a chromium source. The evaluation of the catalytic behavior of a large number of diphosphinoamine (PNP) ligands with various substituents on both the nitrogen and phosphorus atoms followed this discovery.³ It was found that an important factor in the catalyst selectivity (in particular, for 1-octene vs 1-hexene) is the steric bulk on the central nitrogen atom compared to the basicity of the phosphine.^{3d,e} Until now, no efforts were made to systematically quantify this steric effect on the nitrogen atom into a parameter that could be used for further ligand design.

We introduce here the *Effective Tolman-based N-substituent steric parameter* ($\theta_{N\text{-sub}}$) derived from ligand crystallographic and computational data and the synthesis and structural characterization of a platinum compound, [PtCl₂(PNP-*c*Hex)] (1), and a rare chromium compound, [*n*-Pent-NH₃][CrCl₄(PNP-*n*-Pent)]·2C₇H₈ (2) (Figure 1), which contain the diphosphinoamine bidentate ligands, as further proof of concept. The effect on the selectivity is thus illustrated by the systematic increase of

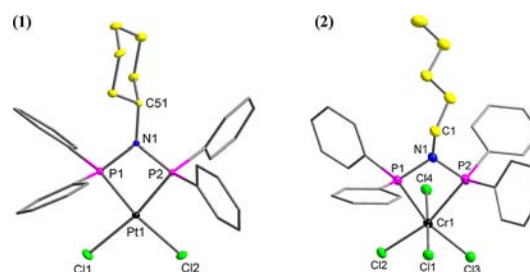
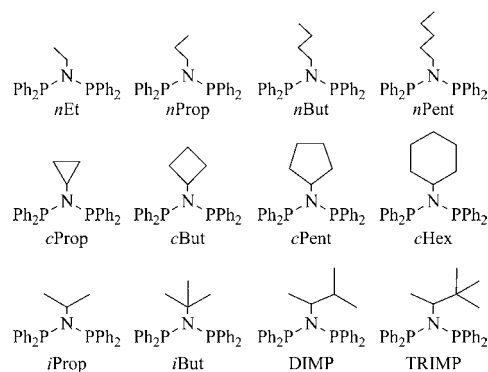


Figure 1. DIAMOND representation of 1 and 2 (hydrogen atoms, solvate molecules, and cations omitted; phenyl rings presented as “stick” models for clarity; ellipsoids set at 50% probability). Selected bond distances and angles are given in the References section.¹⁰

the steric bulk of the substituent on the nitrogen ligand ($\theta_{N\text{-sub}}$) from density functional theory (DFT) calculations on a range of free PNP bidentate ligands (Scheme 1) as well as metal complexes thereof. This is further supported by the X-ray crystallographic data reported herein.

Scheme 1. PNP Ligand Systems with Variation of the Bulkiness at the Nitrogen Atom⁴

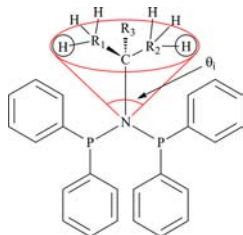
In order to define the $\theta_{N\text{-sub}}$ steric parameter, a tangent line is constructed from the nitrogen atom to the sides of the outermost atoms as defined by their respective van der Waals radii, similar to the original concept introduced by Tolman⁵ (Scheme 2), and the angle is then calculated by using eq 1.

Received: November 26, 2012

Published: February 8, 2013



$$\theta_{N\text{-sub}} = \left(\frac{2}{3}\right) \sum_{i=1}^3 \frac{\theta_i}{2} \quad (1)$$

Scheme 2. Effective Tolman-Based $\theta_{N\text{-sub}}$ Calculation

The structures of the free ligands and metal complexes thereof were determined by X-ray crystallography and compared to the corresponding calculated structures⁶ and with the catalytic data of the corresponding Cr^{III}PNP catalyst systems⁷ (Table 1).

Table 1. Calculated $\theta_{N\text{-sub}}$ (deg) and Selected Ethylene Oligomerization Catalytic Data for Various PNP Ligand Systems

compound	$\theta_{N\text{-sub}}^a$ (deg)	$\theta_{N\text{-sub}}^b$ (deg)	$\theta_{N\text{-sub,Ave}}^c$ (deg)	% 1-C6 ^d	% 1-C8 ^e	% C6 cyclics ^f
nEt	62.9	63.8	63.4	7.3	62.8	10.4
Pt-nEt	62.8	61.8	62.3			
nProp	63.2	64.2	63.9	7.8	60.2	10.9
nBut	63	64.7	63.9	7.8	60.5	10.9
nPent	63.2	64.6	63.9	6.9	58.2	10.1
Cr-nPent	63.5	64.2	63.9			
cProp	68.5	70.9	69.7	8.8	61.4	10.8
cBut	73.1	75.9	74.5	9.3	60.1	10.0
cPent	79.3	82.9	79.3	12.1	63.8	6.7
iProp	80.3		80.3	12.8	69.4	4.1
Pd-iProp	80.4	82.3	81.4			
cHex	81.3	84.5	82.9	14.7	68.2	4.8
Pt-cHex	81.6	83.6	82.6			
Dimp	88.5	83.9	86.2	21.1	66.6	3.6
Pt-Dimp	86.1		86.1			
tBut	97.6	101.6	99.7	30.9	58.4	1.9
Trimp		100.4	100.4	44.4	44.6	1.2

^aCalculated from crystal data. ^bObtained from DFT-optimized structures. ^cAverage from crystal data and calculated structures. ^d% 1-hexene of total liquid product at 45 bar, 60 °C. ^e% 1-octene of total liquid product 45 bar, 60 °C. ^f% C6 cyclic side-product formation of total liquid product 45 bar, 60 °C.

Two crystal structures with different PNP ligands are reported here⁸ with platinum(II) and chromium(III) incorporated as metal centers (Figure 1), while the rest have been published elsewhere and/or are in preparation for publication.⁹ Incorporating data of different metal complexes and free ligands illustrates the consistency in the steric effect of the substituent at the nitrogen atom. It clearly shows that the value of $\theta_{N\text{-sub}}$ does not vary substantially from the free ligand to metal complexes, in spite of using different metals with different ionic radii.

The inclusion of a chromium(III) complex in this study is an obvious one, but crystalline material of its PNP complexes is extremely difficult to obtain. The structure reported here (Figure 1) is thus the first monomeric Cr^{III}PNP complex to date.

Platinum(II) and palladium(II) were used as model complexes in the cases when the chromium complexes were not crystalline.

The steric demand, as modeled with $\theta_{N\text{-sub}}$, has a clear impact on the selectivity. The 1-hexene selectivity increases consistently with increasing $\theta_{N\text{-sub}}$, from just 7% with the least bulky ligands to 44% with the most bulky (Table 1). Meanwhile, the 1-octene/1-hexene ratio decreases almost linearly with increasing $\theta_{N\text{-sub}}$ (Figure 2A), further demonstrating the usefulness of this steric parameter.

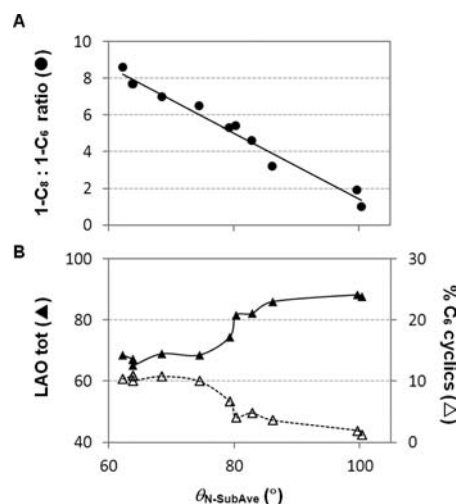
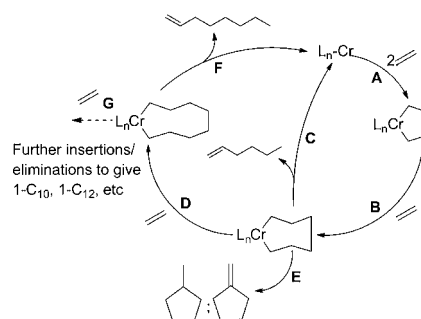


Figure 2. (A) Progressive decrease of the 1-C8/1-C6 ratio correlated to $\theta_{N\text{-sub}}$. (B) Total increase in LAOs (1-C6 and 1-C8;▲) and total percentage decrease of C6 cyclics (Δ) as a result of increasing $\theta_{N\text{-sub}}$.⁷

The 1-octene selectivity, however, does not show a clear trend, with the maximum selectivity obtained for intermediate $\theta_{N\text{-sub}}$ values (Table 1). This is due to the increased propensity for byproduct formation together with 1-octene. In particular, the two C6 cyclics, methylcyclopentane and methylenecyclopentane (as well as C10+ LAOs), are increasingly formed with the least bulky ligands (Table 1). This impacts the total selectivity to the targeted 1-octene and 1-hexene olefins (Figure 2B).

These results can be better understood in the context of the well-established tetramerization mechanism (Scheme 3).^{3a} After formation of the metallacycloheptane species (by pathways A and B), three competing reaction pathways can be followed. Pathway C (reductive elimination) produces 1-hexene and is the only accessible pathway in selective trimerization catalysts. For tetramerization catalysts, pathways D (ethylene insertion to form a metallacyclononane species, leading to 1-octene formation via

Scheme 3. Mechanistic Scheme for Ethylene Tetramerization^{3a}

pathway F) and E (leading to cyclic formation) are competitive with pathway C. The steric bulk of the N-substituent thus clearly affects the relative activation energies of these three pathways. At maximum $\theta_{N\text{-sub}}$, 1-hexene formation is relatively favored. As $\theta_{N\text{-sub}}$ decreases, the 1-octene and cyclic formation pathways are increasingly favored. The reason for this is not well understood; however, we speculate that increased N-substituent bulk forces the P-phenyl groups into the catalytic pocket, thus destabilizing the metallacyclononane species toward reductive elimination.

These results, together with the fact that the computational data and the data obtained from the crystallographic studies agree reasonably well, show the potential of the systematic evaluation of the $\theta_{N\text{-sub}}$ parameter as a tool for ligand design in these oligomerization reactions. It underlines the contribution that DFT calculations, supported by X-ray crystallography and vice versa, can make to ligand design for industrial and other applied reactions and especially in catalysis.¹¹

In conclusion, we have successfully synthesized a range of PNP ligands with variation in the substituents on the nitrogen atom in terms of steric bulk. A steric parameter ($\theta_{N\text{-sub}}$), similar to that used by Tollman⁵ for phosphine ligands, was introduced to describe the steric bulk at the nitrogen atom. This parameter was calculated for the free ligands and different metal complexes thereof and indicated only slight variations. A very specific tendency is observed for the value of $\theta_{N\text{-sub}}$ and 1-hexene selectivity, and a slight increase in 1-octene selectivity is found with increased bulkiness around the nitrogen atom. In reality, it implies a significant reduction in the internalization of the olefin and underlines the subtle steric effects in olefin oligomerization reactions.

■ ASSOCIATED CONTENT

■ Supporting Information

Experimental, characterization, calculation details, and X-ray crystallographic data in CIF format. This material is available free of charge via the Internet at <http://pubs.acs.org>.

■ AUTHOR INFORMATION

Corresponding Author

*E-mail: visserhg@ufs.ac.za (H.G.V.), roodta@ufs.ac.za (A.R.).

Notes

The authors declare no competing financial interest.

■ ACKNOWLEDGMENTS

We thank SASOL, University of the Free State, THRIP, and c*change for supporting this work and Prof G. Steyl for assistance with the computational work.

■ REFERENCES

(1) (a) Alpha Olefins (02/03-4). PERP Report, Nexant Chem Systems. (b) Vogt, D. In *Applied Homogeneous Catalysis with Organometallic Compounds*; Cornils, B., Hermann, W. A., Eds.; Wiley-VCH: Weinheim, Germany, 1996. (c) Dixon, J. T.; Green, M. J.; Hess, F. M.; Morgan, D. H. *J. Organomet. Chem.* **2004**, *689*, 3641–3668. (d) Manyik, R. M.; Walker, W. E.; Wilson, T. P. *J. Catal.* **1977**, *47*, 197–202. (e) Freeman, J. W.; Buster, J. L.; Kudsens, R. D. Preparation of homogeneous catalysts for olefin oligomerization. U.S. Patent 5,856,257, 1999. (f) McGuinness, D. S.; Wasserscheid, P.; Keim, W.; Morgan, D. H.; Dixon, J. T.; Bollmann, A.; Maumela, H.; Hess, F. M.; Englert, U. *J. Am. Chem. Soc.* **2003**, *125*, 5272–5273. (g) Carter, A.; Cohen, S. A.; Cooley, N. A.; Murphy, A.; Scutt, J.; Wass, D. F. *Chem. Commun.* **2002**, 858–859. (h) Agapie, T.; Schofer, S. L.; Labinger, J. A.; Bercaw, J. E. *J. Am. Chem. Soc.* **2004**, *126*, 1304–1305. (i) Briggs, J. R. *J. Chem. Soc., Chem. Commun.* **1989**, *11*, 674–675.

(2) Bollmann, A.; Blann, K.; Dixon, J. T.; Hess, F. M.; Killian, E.; Maumela, H.; McGuinness, D. S.; Morgan, D. H.; Neveling, A.; Otto, S.; Overett, M.; Slawin, A. M. Z.; Wasserscheid, P.; Kuhlmann, S. *J. Am. Chem. Soc.* **2004**, *126*, 14712–14713.

(3) (a) Overett, M. J.; Blann, K.; Bollmann, A.; Dixon, J. T.; Haasbroek, D.; Killian, E.; Maumela, H.; McGuinness, D. S.; Morgan, D. H. *J. Am. Chem. Soc.* **2005**, *127*, 10723–10730. (b) Walsh, R.; Morgan, D. H.; Bollmann, A.; Dixon, J. T. *Appl. Catal., A* **2006**, *306*, 184–191. (c) Rucklidge, A. J.; McGuinness, D. S.; Toozee, R. P.; Slawin, A. M. Z.; Pelletier, J. D. A.; Hanton, M. J.; Webb, P. B. *Organometallics* **2007**, *26*, 2782–2787. (d) Kuhlmann, S.; Blann, K.; Bollmann, A.; Dixon, J. T.; Killian, E.; Maumela, M. C.; Maumela, H.; Morgan, D. H.; Pretorius, M.; Taccardi, N.; Wasserscheid, P. *J. Catal.* **2007**, *245*, 279–284. (e) Blann, K.; Bollmann, A.; de Bod, H.; Dixon, J. T.; Killian, E.; Nongodlwana, P.; Maumela, M. C.; Maumela, H.; McConnell, A. E.; Morgan, D. H.; Overett, M. J.; Pretorius, M.; Kuhlmann, S.; Wasserscheid, P. *J. Catal.* **2007**, *249*, 244–249. (f) Blann, K.; Bollmann, A.; Dixon, J. T.; Hess, F. M.; Killian, E.; Maumela, H.; Morgan, D. H.; Neveling, A.; Otto, S.; Overett, M. J. *Chem. Commun.* **2005**, 620–621. (g) Overett, M. J.; Blann, K.; Bollmann, A.; Dixon, J. T.; Hess, F. M.; Killian, E.; Maumela, H.; Morgan, D. H.; Neveling, A.; Otto, S. *Chem. Commun.* **2005**, 622–624.

(4) Definition of ligand abbreviations: *nEt* = bis(diphenylphosphino)ethylamine, *nProp* = bis(diphenylphosphino)propylamine, *nBut* = bis(diphenylphosphino)butylamine, *nPent* = bis(diphenylphosphino)pentylamine, *cProp* = bis(diphenylphosphino)cyclopropylamine, *cBut* = bis(diphenylphosphino)cyclobutylamine, *cPent* = bis(diphenylphosphino)cyclopentylamine, *Hex* = bis(diphenylphosphino)cyclohexylamine, *iProp* = bis(diphenylphosphino)isopropylamine, *iBut* = bis(diphenylphosphino)isobutylamine, *Dimp* = bis(diphenylphosphino)-1,2-dimethylpropylamine, and *Trimp* = bis(diphenylphosphino)-1,2,2-trimethylpropylamine.

(5) Tolman, C. A. *Chem. Rev.* **1977**, *77*, 313–348.

(6) (a) All DFT calculations were performed with *Gaussian 03*. See: Frisch, M. J. et al. *Gaussian 03*, revision C.01; Gaussian, Inc.: Pittsburgh, PA, 2003. (b) Lee, C.; Yang, W.; Parr, R. G. *Phys. Rev. B* **1988**, *37*, 785.

(7) Catalytic data obtained from refs 3d and 3e and R&D, SASOL Technology.

(8) CCDC 840251 (for **1**) and 840252 (for **2**) contain the supplementary crystallographic data for this paper. These data can be obtained free of charge from the Cambridge Crystallographic Data Centre via www.ccdc.cam.ac.uk/data_request/cif.

(9) (a) Cloete, N.; Visser, H. G.; Roodt, A. *Acta Crystallogr., Sect. E* **2010**, *66*, m51–m52. (b) Cloete, N.; Visser, H. G.; Roodt, A.; Gabrielli, W. F. G. *Acta Crystallogr., Sect. E* **2009**, *65*, o3081. (c) Cloete, N.; Visser, H. G.; Roodt, A.; Dixon, J. T.; Blann, K. *Acta Crystallogr., Sect. E* **2008**, *64*, o480. (d) Engelbrecht, I.; Visser, H. G.; Roodt, A. *Acta Crystallogr., Sect. E* **2010**, *66*, o2881. (e) Engelbrecht, I.; Visser, H. G.; Roodt, A. *Acta Crystallogr., Sect. E* **2010**, *66*, o3322–o3323. (f) Cloete, N. Ethylene tetramerization: structure and reactivity investigation of metal-based catalyst precursors. Ph.D. Dissertation, The University of the Free State, Bloemfontein, South Africa, 2010.

(10) Selected bond distances (Å) and angles (deg) for **1**: Pt1–P1 = 2.2144(8), Pt1–Cl1 = 2.3566(8); P1–N1–P2 = 99.31(13), P2–Pt1–P1 = 71.89(3). Those for **2**: Cr1–P11 = 2.497(3), Cr1–Cl11 = 2.341(2); P11–N11–P12 = 66.71(8), P11–Cr1–P12 = 66.71(8).

(11) (a) Roodt, A.; Visser, H. G.; Brink, A. *Crystallogr. Rev.* **2011**, *17*, 241–280. (b) Schutte, M.; Kemp, G.; Visser, H. G.; Roodt, A. *Inorg. Chem.* **2011**, *50*, 12486–12498. (c) Brink, A.; Roodt, A.; Steyl, G.; Visser, H. G. *Dalton Trans.* **2010**, 39, 5572–5578. (d) Ferreira, A. C.; Crous, R.; Bennie, L.; Meij, A. M. M.; Blann, K.; Bezuidenhout, B. C. B.; Young, D. A.; Green, M. J.; Roodt, A. *Angew. Chem., Int. Ed.* **2007**, *46*, 2273–2275. (e) Haumann, M.; Meijboom, R.; Moss, J. R.; Roodt, A. *Dalton Trans.* **2004**, 1679–1686.